

**Fundamentals of reservoir surface energy as related to  
surface properties, wettability, capillary action, and oil  
recovery from fractured reservoirs by spontaneous  
imbibition**

DE-FC26-03NT15408

Quarterly Report  
01/01/2004 – 3/31/2004

Principal Investigator:  
Norman R. Morrow

May 2004

Submitted by:  
Chemical & Petroleum Engineering  
University of Wyoming  
Dept. 3295, 1000 E. University Ave  
Laramie, WY 82071

## **Disclaimer**

This report was prepared as an account of work sponsored by an agency of the United States Government. Neither the United States Government nor any agency thereof, nor any of their employees, makes any warranty, express or implied, or assumes any legal liability or responsibility for the accuracy, completeness, or usefulness of any information, apparatus, product, or process disclosed, or represents that its use would not infringe privately owned rights. Reference herein to any specific commercial product, process, or service by trade name, trademark, manufacturer, or otherwise does not necessarily constitute or imply its endorsement, recommendation, or favoring by the United States Government or any agency thereof. The views and opinions of authors expressed herein do not necessarily state or reflect those of the United States Government or any agency thereof.

## ABSTRACT

The objective of this project is to increase oil recovery from fractured reservoirs through improved fundamental understanding of the process of spontaneous imbibition by which oil is displaced from the rock matrix into the fractures. Spontaneous imbibition is fundamentally dependent on the reservoir surface free energy but this has never been investigated for rocks. In this project, the surface free energy of rocks will be determined by using liquids that can be solidified within the rock pore space at selected saturations. Thin sections of the rock then provide a two-dimensional view of the rock minerals and the occupant phases. Saturations and oil/rock, water/rock, and oil/water surface areas will be determined by advanced petrographic analysis and the surface free energy which drives spontaneous imbibition will be determined as a function of increase in wetting phase saturation. The inherent loss in surface free energy resulting from capillary instabilities at the microscopic (pore level) scale will be distinguished from the decrease in surface free energy that drives spontaneous imbibition.

A mathematical network/numerical model will be developed and tested against experimental results of recovery versus time over broad variation of key factors such as rock properties, fluid phase viscosities, sample size, shape and boundary conditions. Two fundamentally important, but not previously considered, parameters of spontaneous imbibition, the capillary pressure acting to oppose production of oil at the outflow face and the pressure in the nonwetting phase at the no-flow boundary versus time, will also be measured and modeled. Simulation and network models will also be tested against special case solutions provided by analytic models.

In the second stage of the project, application of the fundamental concepts developed in the first stage of the project will be demonstrated. The fundamental ideas, measurements, and analytic/numerical modeling will be applied to mixed-wet rocks. Imbibition measurements will include novel sensitive pressure measurements designed to elucidate the basic mechanisms that determine induction time and drive the very slow rate of spontaneous imbibition commonly observed for mixed-wet rocks. In further demonstration of concepts, three approaches to improved oil recovery from fractured reservoirs will be tested; use of surfactants to promote imbibition in oil wet rocks by wettability alteration: manipulation of injection brine composition: reduction of the capillary back pressure which opposes production of oil at the fracture face.

## TABLE OF CONTENTS

INTRODUCTION .....	5
Objectives.....	5
TASKS .....	5
EXECUTIVE SUMMARY .....	7
Progress BY TASK.....	7
Task 1.....	7
Introduction .....	7
Experimental.....	8
Results and Discussion .....	8
Task 2.....	10
Introduction .....	10
Experimental.....	10
Task 3.....	14
Introduction .....	14
Experimental.....	14
Results and Discussion .....	15
Task 4.....	18
Introduction .....	18
Experimental.....	18
Results and Discussion .....	19
Task 5.....	23
Introduction .....	23
THEORY.....	23
CONCLUSIONS.....	27
REFERENCES .....	27

# INTRODUCTION

## Objectives

The long-range objective of this project is to improve oil recovery from fractured reservoirs through improved fundamental understanding of the process of spontaneous imbibition by which oil is displaced from the rock matrix into the fractures. Spontaneous imbibition is fundamentally dependent on the surface energy. An initial objective is to determine the surface energy and relate the dissipation of surface energy to the mechanism of spontaneous imbibition. A parallel objective is to model the mechanism of spontaneous imbibition by a combination of network analysis and numerical modeling. Also fundamentally important, but not previously considered, parameters of spontaneous imbibition, the capillary pressure acting to oppose production of oil at the outflow face and the pressure in the nonwetting phase at the no-flow boundary (in effect within oil in the non-invaded zone of the rock matrix) versus time, will also be measured and compared with values predicted by the mathematical model. The next objective is to measure surface energy and related spontaneous imbibition phenomena for mixed-wettability rocks prepared by adsorption from crude oil. The dissipation of surface free energy must then be related to oil production at mixed-wet conditions. The final objective is to apply the results of the project to improved oil recovery from fractured reservoirs in three ways: reduction of the capillary force that opposes oil production at the fracture face; change in wettability towards increased water wetness; identification of conditions where choice of invading brine composition can give improved recovery.

## TASKS

### **Budget period 1, July 1, 2003 through June 30, 2005 – Ideas and Concept development: Fundamentals of Spontaneous Imbibition**

*Task 1. Work of displacement and surface free energy.* Obtain complementary sets of capillary pressure drainage and imbibition data and data on changes in rock/brine, rock/oil, and oil/brine interfacial areas with change in saturation for drainage and imbibition for at least two rock types (sandstone and carbonate). Determine free-energy/work-of-displacement efficiency parameters for drainage and imbibition for at least two rock types so that changes in rock/wetting phase/nonwetting phase surface areas can be closely estimated from capillary pressure measurements.

*Task 2. Imbibition in simple laboratory and mathematical network models.* Study imbibition in at least three simple tube networks that can be modeled analytically to establish and/or confirm fundamental aspects of the pore scale mechanism of dynamic spontaneous imbibition with special emphasis on determining how spontaneous imbibition is initiated and the key factors in how the saturation profile develops with time. Incorporate rules developed from laboratory measurements on relatively simple networks into the design of a computational network model. Use the network model to obtain an account of the mechanism by which imbibition is initiated, the saturation profile is developed, and the rate of spontaneous imbibition in terms of the dissipation of surface free energy that accompanies change in saturation.

**Task 3.** *Novel observations on fluid pressures during imbibition and the mechanism of non-wetting phase production at the imbibition face.* Make novel observations on the imbibition mechanism including details of the mechanism of oil production at the outflow rock face and the change in the nonwetting phase pressure at the no-flow boundary of the core during the course of spontaneous imbibition for at least 16 distinct combinations of rock/ fluid properties.

**Task 4.** *Network/numerical model and new imbibition data.* Develop a numerical simulator specifically designed for spontaneous imbibition. Incorporate the network model to obtain a network/numerical model that includes matching the measured pressure in the nonwetting phase at the no-flow boundary, and the pressure that opposes production of oil at the open rock face. Imbibition data will be obtained for at least 10 rocks with over six-fold variation in permeability, and at least 6 orders of magnitude variation in viscosity ratio, and at least 10 variations in sample size, shape, and boundary conditions.

**Task 5.** *Comparison with similarity solutions.* Compare results given by simulation with special case analytic results given by similarity solutions for spontaneous imbibition for at least five distinct cases of rock and fluid properties.

**Budget Period 2, July 1, 2005 through June 30, 2008 - Demonstration of concept:  
Application to mixed wettability rocks and improved oil recovery from fractures reservoirs.**

**Task 6.** *Rock preparation and Work of displacement and surface areas*

Obtain a range of rock types and identify and obtain crude oils that induce stable mixed wettability. Prepare at least 25 rocks with mixed wettability through crude oil/brine/rock interactions.

Determine work of displacement for drainage and imbibition and measure the variation in rock/brine, rock oil, and oil/brine interfacial areas during the course of drainage and imbibition for at least two examples of mixed wettability.

**Task 7.** *Novel imbibition measurements on mixed-wet rock and network models.* Obtain, for at least six mixed-wet rocks, spontaneous imbibition data that includes measurements of the nonwetting phase pressure at the no-flow boundary, observations on the capillary pressure that resists production at the open rock face.

**Task 8.** *Application of network/numerical model to mixed wet rocks.* Use network models to relate dissipation of surface energy to rate of spontaneous imbibition and to account for the frequently observed induction time prior to onset of spontaneous imbibition into mixed wettability rocks.

**Task 9.** *Increased oil recovery by spontaneous imbibition.* The mechanism of increased recovery from mixed wet rocks by use of surfactants that promote spontaneous imbibition by favorable wettability alteration will be investigated for at least four distinct examples of crude oil/brine/rock/surfactant combinations.

The mechanism of increased recovery by manipulation of brine composition will be investigated for at least four crude oil/brine/rock combinations.

Addition of very low concentrations surfactants to the imbibing aqueous phase will be explored as a means of increasing the rate of oil recovery by reducing the capillary forces which resist production of oil at the fracture face. At least twelve combinations of rock and fluid properties including both very strongly wetted and mixed wet rocks will be tested.

## **EXECUTIVE SUMMARY**

A technique has been developed to image and measure changes in rock/fluid and fluid/rock interfacial areas in sandstone and limestone. Preliminary results are reported on imbibition by consolidated bead packs. A novel combination of measurements of saturation change, location of the invasion front and the dead end pressure in the nonwetting phase is reported for oil/air and water/oil imbibition. Recovery of 4 cP oil by imbibition of wetting phase ranging from 1 to 1650 cP has been measured. An analytical solution for saturation change by spontaneous imbibition is presented.

## **PROGRESS BY TASK - BUDGET PERIOD 1**

### **Task 1. *Work of displacement and surface free energy.***

The aim of this research is to understand the mechanism of the spontaneous imbibition, a process which can be of key importance in oil production from fractured reservoirs. During the process of spontaneous imbibition, the surface free energy of the system is converted to work of displacement, for example in the recovery of oil. The method proposed in this work utilizes thin section analysis from different core samples to determine fluid saturation and surface areas after solidification of epoxy resin. This information relates change in surface free energy to saturation.

### **Introduction**

Changes in surface areas between solid, oil and water take place during the process of displacement of oil from an oil reservoir. Multi phase flow and mass transfer are intricately related to the surface area between the three phases. Therefore for a fundamental understanding of displacement, i.e. imbibition and drainage, the accompanying change in surface energy during these processes must be understood. Morrow (1970), measured changes in surface energy during drainage using thin section analysis for a packing of beads of uniform size. Epoxy resins of two different colors were used to simulate the wetting and the non-wetting phase. Indirect method of using interfacial tracer to determine the interfacial areas have been tried by a few researchers (Jain et al., 2003, Kim et al. 1997, Gladkikh et al., 2003). Bradford and Leij (1997) discuss theoretical ways of predicting changes in surface energy in soil samples.

Wetting state of the solid, i.e. oil-wet, water wet or mixed wet, has a significant impact on the interfacial areas and hence recovery from a particular reservoir. Bradford and Leij (1997), Jain et al. (2003) and, Gladkikh et al. (2003) discuss ways of altering the wettability of the sample by using different amounts of silanes. Bradford and Leij (1997) makes theoretical predictions for the changes in interfacial areas during imbibition and drainage whereas Jain et al. (2003) and Gladkikh et al. (2003) rely on the tracer technique to estimate the same quantities.

In our research, actual core samples from outcrops are used for analysis. This involves a greater degree of complication as compared to the work done by other researchers (Morrow, 1970; Jain et al., 2003; Kim et al., 1997, Gladkikh et al., 2003; Bradford and Leij, 1997; Scheafer et al., 2000a; Sheaffer et al., 2000b) who worked with unconsolidated media (either bead pack or soil). Preliminary analysis will be done for Berea sandstone and a limestone sample. The experimental method is very similar to one discussed by Morrow (1970) that employs thin section analysis.

## **Experimental**

### Imaging of fluid distribution for drainage

As mentioned in the previous quarterly, the change in surface free energy is related to the fluid saturation in the core. To study the fluid distribution of the two phases, i.e. wetting and the non wetting phase, a colored epoxy resin was used. Araldite 502 mixture as a resin was used for the study. During centrifugation, the high viscosity of the epoxy resin limited the residual saturation of the wetting phase to a high value (~ 57% for Berea Sandstone). Hence, for future studies, it has been decided to switch to a low viscosity Spurr's Resin kit to obtain a lower residual saturation when centrifuged. The ingredients of the epoxy resin were:

1. 10 g of ERL 4206 – Vinyl Cyclohexene Dioxide (VCHD)
2. 4 g of DER 736 – Diglycidyl Ether
3. 26 g of NSA – Nonenyl Succinic Anhydride
4. 0.3 g of DMAE - Dimethylaminoethanol

The procedure remains essentially unchanged from that described in the second quarterly report.

## **Results and Discussion**

Two phase fluid distribution for sandstone (Berea) was obtained using the Araldite epoxy mixture. As mentioned earlier, the high viscosity of this epoxy mixture limited our efforts to obtain low residual saturation for the wetting phase. Results covered a range of saturation from 58 % to 76 % for the four thin sections that were analyzed. Fig. 1 shows a picture of the sample, with the two phases, that was analyzed. Further analysis on the surface area measurement is currently underway.

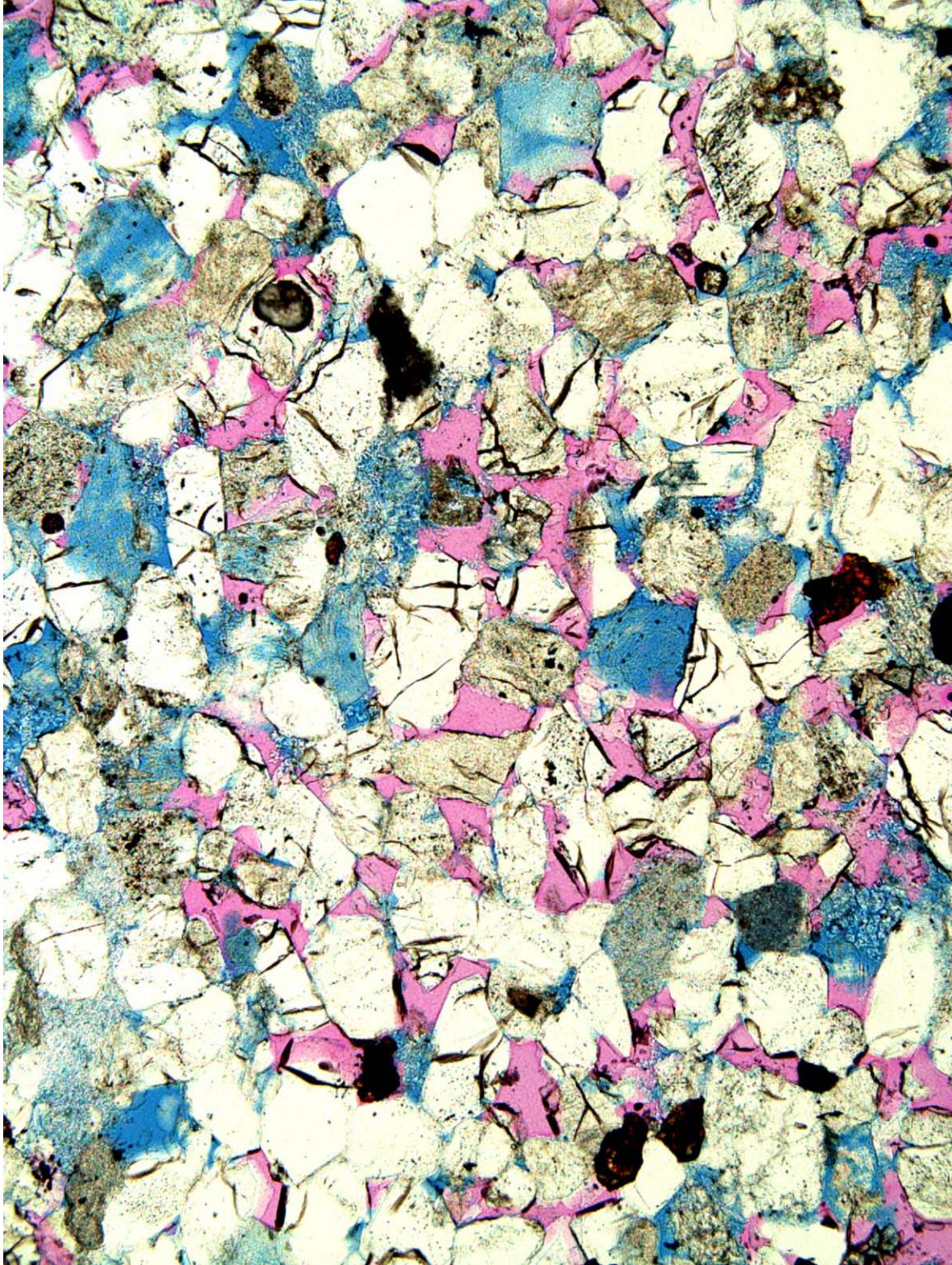


Fig. 1.1 Berea Sandstone sample showing two phases

## Task 2. Imbibition in simple laboratory and mathematical network models.

### Introduction

Imbibition properties for a wide range of viscosity ratios and for different matched viscosities are presented for various consolidated bead packs (glass). The rate of recovery was a strong function of the viscosity of the wetting phase (the viscosity of the non wetting phase was kept constant). The dimensionless time ( $t_D$ ), used to scale for the interfacial tension, two phase viscosities, permeability, and porosity, did not provide close correlation for the different samples. However it was observed that for the linear portion of the recovery curve (time required for the wetting phase to reach the no flow boundary) a consistent pattern between the aqueous phase viscosity and dimensionless time ( $t_D^*$ ) existed. Visual examination of the uptake of brine by spontaneous imbibition revealed the presence of heterogeneity that impacted the displacement pattern at very high rates.

### Experimental

#### Properties of the core sample

Properties of the cores formed by lightly fusing glass beads are listed in Table 2.1.

Table 2.1

	Permeability, Darcy	Porosity, %	Pore Volume, ml
Core # 1*	4.4	37.9	21.05
Core # 2*	4.4	36.5	20.77
Core # 3*	4.1	35.9	19.88
Core # 4	3.6	35.9	21.87
Core # 5	3.9	37.3	23.65
Core # 6	3.4	38.0	21.05

\* 2.25 inch size core holder was used as compared to 1.75 inch holder for making other cores

The cores thus prepared are drilled from the fused bead matrix, using a 1.5 inch drill bit. The core was then dried at 110 °C. Potters Ballotini® impact beads were used for preparing the core. A high purity quartz holder was used as a mold. It was observed that the size of the holder did have an effect on the permeability of the core obtained (Table 1). The quartz holder was cut into two pieces that were tied by stainless steel wire to hold the unconsolidated beads in place. After fusing the beads, the wire was cut and the core was removed from the holder. A ceramic tile was placed below the core holder to prevent damage to the base of the core holder during sintering.

#### Recovery of oil from consolidated bead packs for different viscosity ratios

The consolidated core was saturated with a heavy mineral oil (viscosity 181.5 cP). To viscosify the wetting phase, different mixtures of glycerol-distilled water mixtures were used. During the various runs only the viscosity of the aqueous (wetting) phase is changed for different

experiments. This provides a wide range of viscosity ratio over which to test the dimensionless time  $t_d$ .

$$t_d = \sqrt{(k/\Phi)} * (\sigma / \sqrt{(\mu_w \mu_{nw})}) * (1/L_c^2) * t \quad (2.1)$$

where,  $t$  is the actual time

$K$  is the permeability

$\Phi$  is the porosity

$\sigma$  is the interfacial tension

$\mu_w, \mu_{nw}$  are the viscosities of the wetting and non wetting phase respectively

$L_c$  is the characteristic length of the core (in the case all faces open to imbibition) in the results presented, given by

$$L_c = r * L / \sqrt{(4 * r^2 + 2 * L^2)} \quad (r = \text{radii and } L = \text{length of the sample}) \quad (2.2)$$

The properties of the two phases were measured and are listed in table 2.2.

Table 2.2.

	Visc. Glycerol-water (wetting phase), cP	Visc. Mineral oil (non wetting phase), cP	IFT dyn/cm	Visc. Ratio	Time to NFB, $T_d^*$
Core # 1	12.2	181.5	35.74	14.9	134
Core # 2	136.2	181.5	31.21	1.3	348
Core # 3	3.3	181.5	40.79	55.0	213
Core # 4	23.6	181.5	34.12	7.7	67
Core # 5	17.6	181.5	34.80	10.3	23
Core # 6	1.0	181.5	50.89	181.5	30

Figure 2.1 shows the recovery curves obtained for spontaneous imbibition in glass beads along with an imbibition curve for Berea sandstone for reference. As is evident from the correlation using the dimensionless group,  $t_D$  does not provide close correlation of the data obtained so far. For a viscosity ratio (viscosity of oil/viscosity of glycerol mixture) of 10 or less it is observed that the imbibition rate is considerably higher than the other cases. It might be that, as the viscosity ratio goes up the efficiency of displacement is increased (see curves for wetting phase viscosities of 23.6 cP and 136.2 cP as compared to other viscosities in figure 1 or figure 2).

As is obvious from figure 2.1 and figure 2.2 the recovery curve from spontaneous imbibitions consists of two parts, a linear portion and a relatively flat portion. We hypothesize that the linear portion corresponds to the time for the wetting phase to reach the hypothetical no flow boundary (NFB) inside the core. The data obtained using the linear portion of the normalized curve (Figure 2.2) was used to determine  $T_D^*$ , the time required for the aqueous (wetting) phase to reach the hypothetical no flow boundary. This data is obtained from Figure 2.3 and can be plotted as a function of the viscosity ratio as shown in Figure 2.4.

For perfect correlation of the data shown in Figure 4, it would lie on a straight line, probably pointing towards inadequacy of the correlation in this case. Observations of imbibition into a core set in liquid indicated that the results may be strongly impacted by core scale heterogeneities. The effect of these heterogeneities is accentuated by the very fast imbibition rates exhibited by highly permeable bead packs. Results were very much more consistent for sandstone (see task 4)

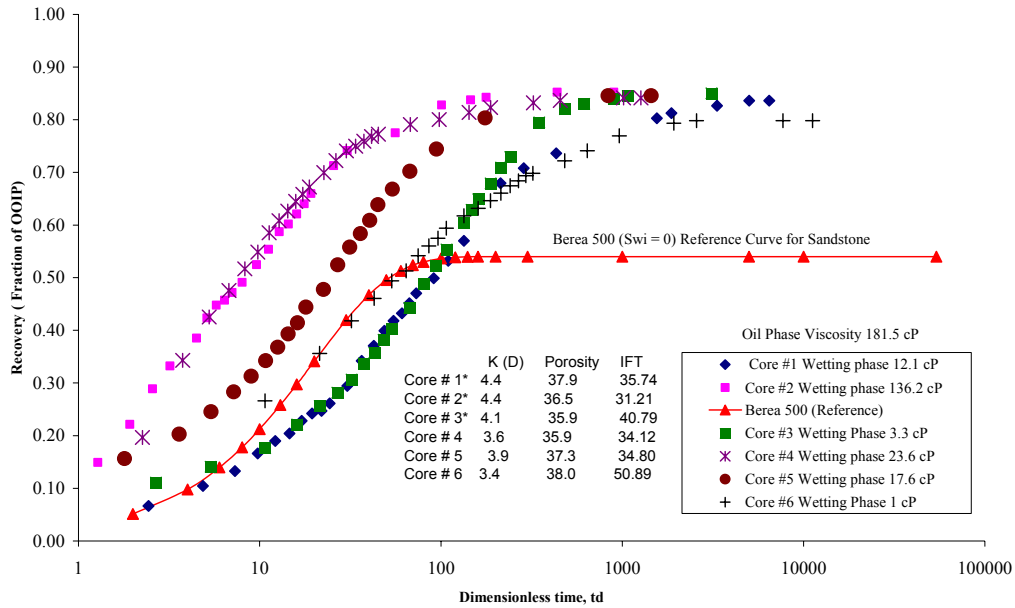


Fig. 2.1 Variability in oil recovery for scaled imbibition for preliminary results on cores formed by consolidation of glass beads

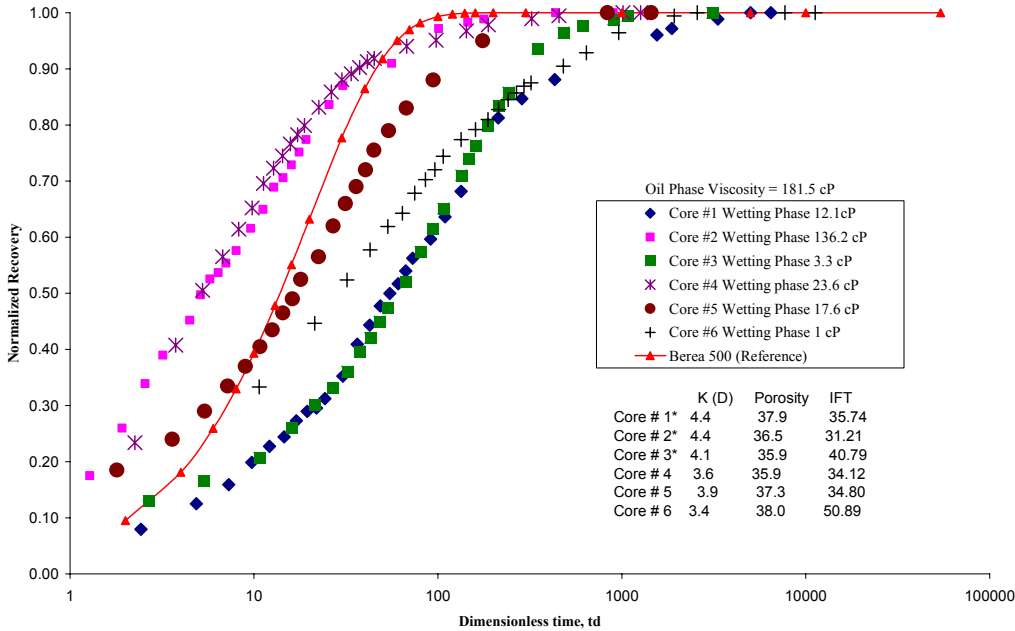


Fig. 2.2 Normalized oil recovery for scaled imbibition for preliminary results on cores formed by consolidation of glass beads

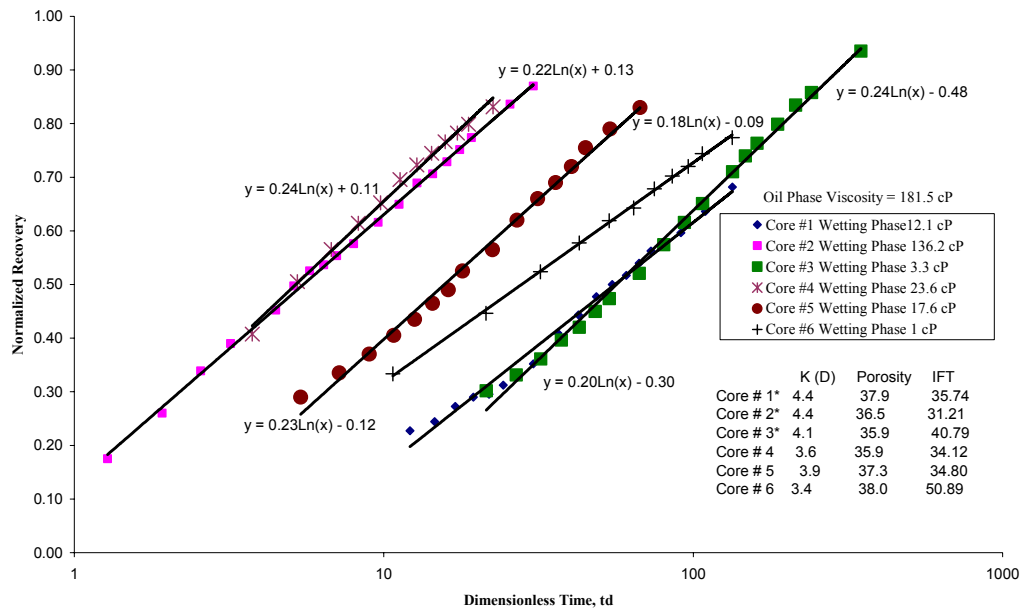


Fig. 2.3 Time ( $t_D^*$ ) for the wetting phase to reach the assumed no flow boundary (NFB) this is the linear part of the normalized recovery curve.

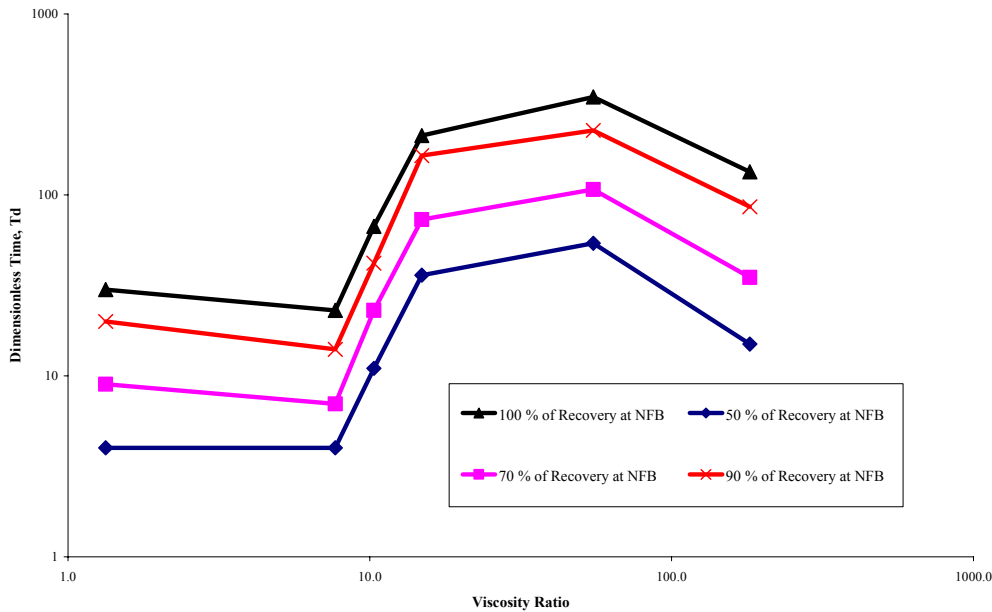


Fig. 2.4 Effect of viscosity ratio on dimensionless time required to reach the no flow boundary (NFB), based on departure from linearity.

### Task 3. Novel observations on fluid pressures during imbibition and the mechanism of non-wetting phase production at the imbibition face.

#### Introduction

Oil/water and air/oil imbibition results have been obtained for Berea sandstone.

#### Experimental

Eight Berea sandstone core samples, 3.8 cm in diameter and about 7 cm in length, were selected. Permeability ranged from  $0.065 \mu\text{m}^2$  to  $1.094 \mu\text{m}^2$  and porosity from 17% to 22%. The cylindrical surface and one end-face of each core were sealed with transparent epoxy resin. One end of a Nylon tube (inner diameter of 1.5 mm and outer diameter of 3 mm) was embedded a short distance into the core at the otherwise sealed end. The other end was connected to a pressure transducer. The tube and the connected transducer space were filled with oil.

Four water/oil and four oil/air imbibition tests were performed (Table 3.1). All experiments were conducted at ambient conditions,  $21^\circ\text{C}$  and atmospheric pressure ( $79 \text{ kPa}$ ). Soltrol 220<sup>®</sup>, of  $0.0038 \text{ Pa}\cdot\text{s}$  viscosity, was used as the oil phase. Polar impurities were removed from the refined oil by flow through silica gel and alumina. In the water/oil experiments the aqueous phase was 10,000 ppm NaCl brine with  $0.00102 \text{ Pa}\cdot\text{s}$  viscosity. The interfacial tension was  $48.9 \text{ mN/m}$ . The surface tension of oil/air was  $25.9 \text{ mN/m}$  and the viscosity of air was  $0.000018 \text{ Pa}\cdot\text{s}$ . In each imbibition experiment, volumetric production, imbibition front position, and NWP dead end pressure were measured simultaneously by techniques described below.

Table 3.1 Core and fluid properties and measured characteristics of imbibition tests.

COUCSI	OIL / WATER				AIR / OIL			
$\mu_{nw}/\mu_w$	0.0038 Pa.s/0.00102 Pa.s				0.000018 Pa.s/0.0038 Pa.s			
$\sigma$	48.85mN/m				25.87mN/m			
CORE	H8O	H2O	M3O	L8O	H8A	H4A	M3A	L5A
$d$ (cm)	3.796	3.794	3.792	3.797	3.789	3.789	3.793	3.8
$L$ (cm)	6.864	6.18	7.493	6	7.12	7.523	7.365	6.806
$K$ ( $\mu\text{m}^2$ )	1.094	1.048	0.681	0.065	1.054	0.973	0.503	0.07
$\Phi$	0.221	0.22	0.208	0.171	0.219	0.217	0.202	0.172
$T_{\text{FAB}}$ (s)	9000	7500	17000	53500	25500	28400	50000	240000
$T_{\text{ep}}$ (s)	30000	22800	54000	150000	70000	75000	130000	547300
$S_{w0}$	0.5	0.5	0.52	0.43	0.5	0.5	0.52	0.53
$P_{\text{end}}$ (kPa)	3.140	3.120	4.830	9.080	1.950	2.240	2.700	4.600

#### Water/oil imbibition

In the water/oil experiments, the core was positioned with the open face up. The recovery was determined from the volume of produced oil collected in an inverted closed funnel above the core (Fig.3.1). A series of electrodes were embedded in the core. The distance of frontal advance was detected from the onset of electrical conductivity when the brine front contacted a particular electrode.

### ***Oil/air imbibition***

In the oil/air experiments, the core was immersed in oil contained in a beaker with the open face down (Fig. 3.1). The beaker was set on a balance with the pressure sensing tube fixed to a stand. The recovery was determined from the incremental loss in weight resulting from imbibition of oil into the core. The ratio of the outside radius of the nylon tube connected to the transducer to the inside radius of the beaker and decrease in the oil level in the beaker were both so small that the influence of buoyancy on recovery could be neglected. However, for measurements that lasted for more than about one day, a small correction was made for loss of oil by evaporation. In these tests, the distance advanced by the oil was obtained by direct observation of the invading front through the transparent resin coating.

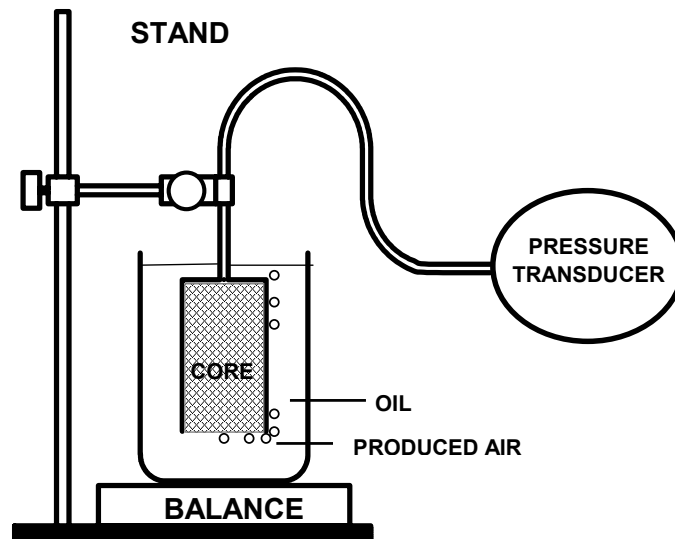


Fig. 3.1 Apparatus for simultaneous measurements of production, location of the front, and dead end pressure during oil/air spontaneous imbibition.

### ***Capillary pressure at the displacement front***

Imbibition tests were also run on a high permeability rock with a lower permeability rock set at the end face in order to estimate the capillary pressure at the imbibition front. Further details are given with the results.

## **Results and Discussion**

### ***Effect of gravity***

The effect of gravitational forces acting over the core length is generally very small compared to capillary forces. Imbibition tests performed with the open end of the core facing either upward or downward showed very little difference in recovery behavior.

### Mode of nonwetting phase production

It was observed that the mode of NWP production was very different for the two fluid pairs. For imbibition of water, oil is produced almost instantaneously after immersion in brine. The oil appears as numerous small drops which tend to coalesce at the open face. For oil/air imbibition, there is no immediate production of air. When air bubbles do appear, they come from only one or two points on the open face.

### Water/oil imbibition

Results presented for Core H8O in Fig. 3.2 are typical of the four data sets obtained for water/oil imbibition. During the frontal flow period, the volume of water imbibed,  $Q_w$ , the distance advanced by the imbibition front,  $x_f$ , and the end pressure,  $P_{end}$ , were recorded.  $P_{end}$  rose quickly for the first 60 seconds. It then remained constant at about 3.140 kPa until the front reached the end of the core (after 9000 seconds). The ratio of  $Q_w/V_\phi$  to  $x_f/L_c$  (the average saturation behind the front) was 0.42 until the imbibition front reached the end of the core. This behavior is consistent with the existence of a self-similar displacement. Both the fractional pore space filled ( $Q_w/V_\phi$ ) and the fractional distance imbibed ( $x_f/L_c$ ) were proportional to the square root of time (Fig.3.2).

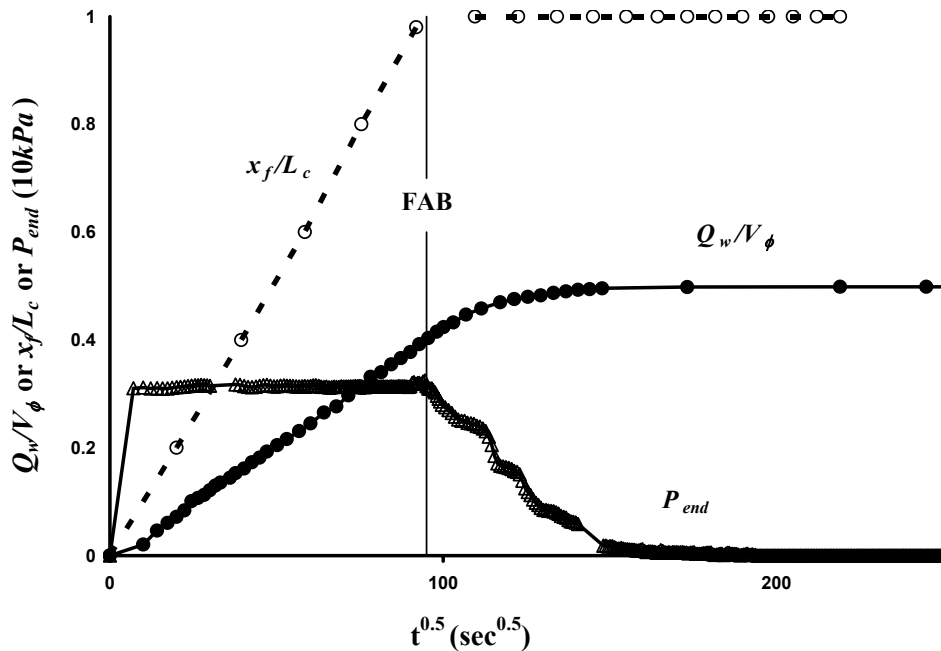


Fig. 3.2 Typical experimental results for water displacing oil versus square root of time (Core H8O).  $Q_w/V_\phi$  is the fractional saturation of total pore space filled by the invading wetting phase.  $x_f/L_c$  is the fraction of the bulk volume of the core (proportional to fraction of pore volume and also the fractional distance) through which the front has advanced as determined by electrical contact.  $P_{end}$  is the pressure measured at the dead end. FAB (front at boundary) indicates the time when the front arrives at the dead-end. The distance advanced by the front and the production prior to FAB are proportional to the square root of time.

### Post contact behavior

After the front reached the end of the core, the rate of oil recovery decayed away from the square root of time relationship. The pressure measured at the closed end ( $P_{end}$ ) decreased and eventually dropped to zero about 30,000 seconds after the start of imbibition. We are not sure why. The final recovery was 50%.

Qualitatively comparable results were obtained for three other Berea sandstones with permeability ranging from 0.065 to 1.048  $\mu m^2$  (see Table 3.1). All end pressures eventually dropped to zero after the front reached the end of the core.

### Oil/air imbibition

Example results for oil/air imbibition in Core H8A are presented in Fig. 3.3. After the start of imbibition,  $P_{end}$  rose to a peak value of 2.118 kPa at 150 seconds and then dropped to 1.980 kPa. The initial build up in pressure corresponded to compression of the air initially contained in the core. No air was produced until about 3% pore volume had been invaded for the high permeability cores. After the drop in pressure that followed the very short initial compression stage,  $P_{end}$  remained constant whilst the imbibition front traversed the core. In contrast to water/oil, the pressure decreased only slightly after the front reached the closed end, maybe because of the compressibility of the air. Apart from the early time behavior, the overall increase in oil saturation and the distance of invasion were, as for water/oil imbibition, proportional to the square root of time during the frontal flow period. When the front reached the closed end of the core 25,500 seconds after the start of imbibition, the NWP recovery, given by  $Q_w/V_\phi$ , was 42%.

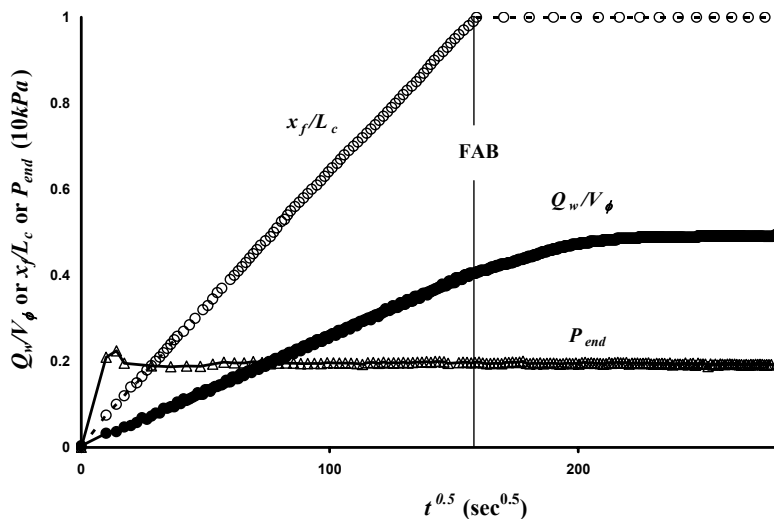


Fig. 3.3 Typical experimental results for imbibition of oil against air versus square root of time (Core H8A). The distance advanced (determined visually) and the production prior to FAB are proportional to the square root of time

### ***Post contact behavior***

After the frontal flow period, the rate of recovery decayed and had almost ceased after 80,000 seconds, by which time the recovery had risen to 50%. After the front had reached the end of the core, the end pressure dropped by about 1% (about 0.020 *kPa*) even though no air was being produced.

Qualitatively comparable oil/air results were obtained for all four Berea sandstones with permeability ranging from 0.070 to 0.973  $\mu\text{m}^2$ . During the post contact period, the decrease in  $P_{end}$  tended to be slightly more for the less permeable cores. For the least permeable core, Core L5A (0.070  $\mu\text{m}^2$ ),  $P_{end}$  had decreased by 2% after 307,300 seconds.

## **Task 4. Network/numerical model and new imbibition data.**

### **Introduction**

Laboratory work of oil recovery with glycerol as the aqueous phase viscosifying agent was the next step under this task. Use of glycerol as a viscosifying agent for aqueous solutions was used to investigate oil recovery by spontaneous imbibition into sandstone at very strongly water-wet conditions for aqueous phase viscosities ranging from 1-1650 cP. One data set for unmatched viscosity was obtained with the oil viscosity fixed at 4 cP. Use of the geometric mean viscosity (Ma et al., 1997) in the definition of dimensionless time gave satisfactory correlation of data. An overall slight trend of increase in dimensionless time with viscosity ratio within the correlated data became accentuated with increase in viscosity ratio. Residual oil saturation attained by spontaneous imbibition showed an overall decrease with increase in viscosity of the aqueous phase. All measurements were made at ambient temperature

### **Experimental**

#### **MATERIALS**

##### **Liquids**

Glycerol ( $\text{CH}_2\text{OHCHOHCH}_2\text{OH}$ ), supplied at 99.5 % purity by EMD sciences, was utilized to viscosify the aqueous phase. Synthetic seawater (Table 4.1) was used in preparation of glycerol/brine solutions in order to avoid possible problematic aqueous phase/rock interactions associated with ionic strength. Mixtures of seawater and glycerol were prepared based on constituent weight percent. Ionic strength was not adjusted for the addition of glycerol and so decreased with decrease in water content. Before use in imbibition experiments, the aqueous phase was evacuated for 3 hours to minimize the possibility of the evolution of gas during the imbibition process. Specific aqueous phase properties were measured directly before a spontaneous imbibition test.

The oil phase was composed of Soltrol 220 (hereafter described as low viscosity oil, LVO) of 3.9 cP viscosity and 0.782  $\text{g}/\text{cm}^3$  density. Polar contaminants were removed from the mineral oils by either contacting the oil with alumina and silica gel in packed columns (LVO) or by suspension followed by filtration (HVO). Each mixture was evacuated for about 3 hours to

remove any dissolved gas prior to measurement of the physical properties of a specific mixture.

Table 4.1 Synthetic Seawater Composition and Properties		
$\rho_w = 1.0238 \text{ g/cm}^3, \mu_w = 1.1 \text{ cP}$		
NaCl	28.0000	g/L
KCl	0.9350	g/L
MgCl <sub>2</sub> *6H <sub>2</sub> O	5.3625	g/L
CaCl <sub>2</sub>	1.1900	g/L
NaN <sub>3</sub>	0.1000	g/L
TDS	35.5875	g/L

### Sandstone

Cylindrical Berea sandstone cores with a nominal diameter,  $d$ , of 3.81 cm and a nominal length,  $l$ , of 6.35 cm were cut from Berea sandstone blocks. The cores were washed, dried at ambient temperature for one day and then oven dried at 105 °C for two days. Subsequently, nitrogen gas permeability,  $k_g$ , was measured in a Hassler-type core holder at a confining pressure of 300 psi. The permeability to nitrogen varied between 63 to 72 md. Core porosity was calculated from the increase in mass that resulted from saturation of a core sample with oil. The rock porosity was around 17 %. Core properties are provided with the individual data sets. The characteristic length,  $L_c$ , for each core for all faces open to imbibition is given by (Zhang et al., 1996)

$$L_c = \frac{ld}{2\sqrt{d^2 + 2l^2}} \quad (4.1)$$

All cores were cut to nominally the same size and so had essentially the same characteristic length of about 1.24 cm.

In all experiments, the initial water saturation was 0 %, a condition which has been adopted as a convenient reference starting condition in previous studies (Mattax and KYTE, 1962; Zhang et al., 1996; Ma et al., 1999). The boundary condition for each core was all faces open. Oil recovery versus time was measured in standard glass imbibition cells at ambient temperature.

### Results and Discussion

Results for the unmatched viscosity were correlated by the modified Ma et al. scaling group

$$t_D = t^* \sqrt{\frac{k}{\phi}} * \frac{\sigma}{\mu_g} * \frac{1}{L_c^2} \quad (4.2)$$

## SPONTANEOUS IMBIBITION

Core and fluid properties are listed in Table 4.2. The aqueous phase viscosity for these spontaneous imbibition experiments covers the entire range from 1.1 cP for seawater to 1646.6 cP for glycerol.

Core #	L <sub>C</sub> cm	k <sub>g</sub> md	$\Phi$ %	$\sigma_{ow}$ dyn/cm	$\rho_{ap}$ g/cm <sup>3</sup>	$\mu_{ap}$ cP
C3-1	1.247	63.5	16.9	48.9	1.026	1.1
C1-1	1.242	62.3	16.9	39.8	1.121	4.4
C3-9	1.242	70.5	16.9	37.6	1.152	8.7
C1-2	1.230	64.5	16.9	35.3	1.172	15.2
C3-6	1.241	66.7	17.0	34.4	1.186	21.8
C3-8	1.241	62.7	17.0	32.9	1.200	39.5
C3-7	1.237	64.5	16.9	32.1	1.211	59.4
C1-3	1.242	62.7	16.8	31.2	1.222	99.8
C1-16	1.237	69.9	17.3	30.6	1.243	185.0
C1-20	1.239	71.2	16.8	28.3	1.255	826.9
C1-25	1.238	71.5	17.4	27.7	1.261	1646.6

The imbibition curves for recovery of 4 cP oil for different aqueous phase viscosities are shown in Fig. 1. The rates of recovery decreased systematically by over 2 ½ orders of magnitude with increase in aqueous phase viscosity. The data were closely correlated by plots of oil recovery versus dimensionless time,  $t_D$ , (see Fig. 4.1b). However the slopes of the scaled curves decreased slightly with increase in aqueous phase viscosity and also show a small but systematic increase in  $t_D$  with increase in aqueous phase viscosity. Final oil recoveries tended to increase with viscosity ratio, apart from a plateau in the viscosity ratio range of 4 to 60 (see Fig. 4.1c).

The trends shown in Fig. 4.1 may be related to subtle changes in the displacement mechanism. The increase in displacement efficiency with viscosity ratio (Fig. 4.1c) may be related to the improved mobility ratio or perhaps to the effect of the aqueous phase on the microscopic mechanism of displacement whereby snap-off is retarded by the viscosity of the aqueous phase. In comparable studies of recovery of refined oil by imbibition of brine, final oil recovery was independent of oil viscosity for values ranging from 1 to 160 cP (Zhang et al., 1996).

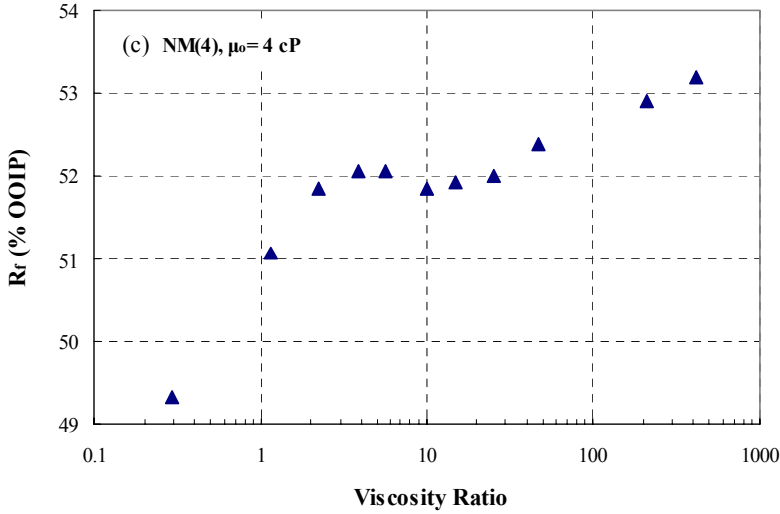
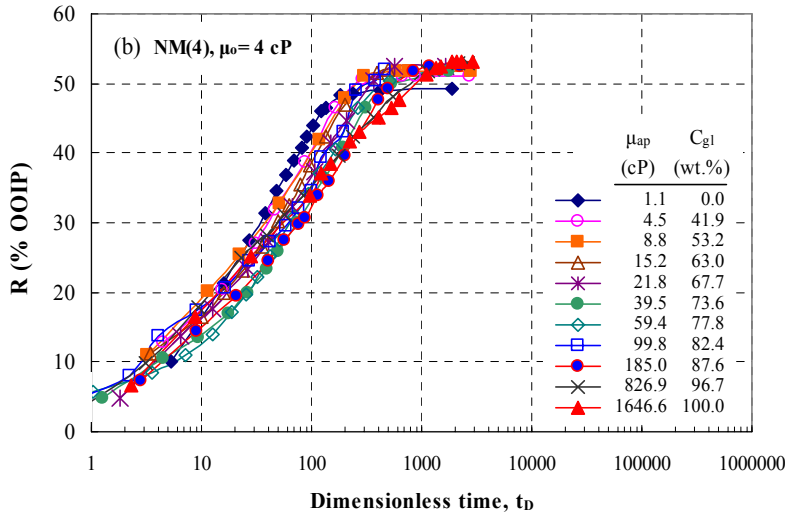
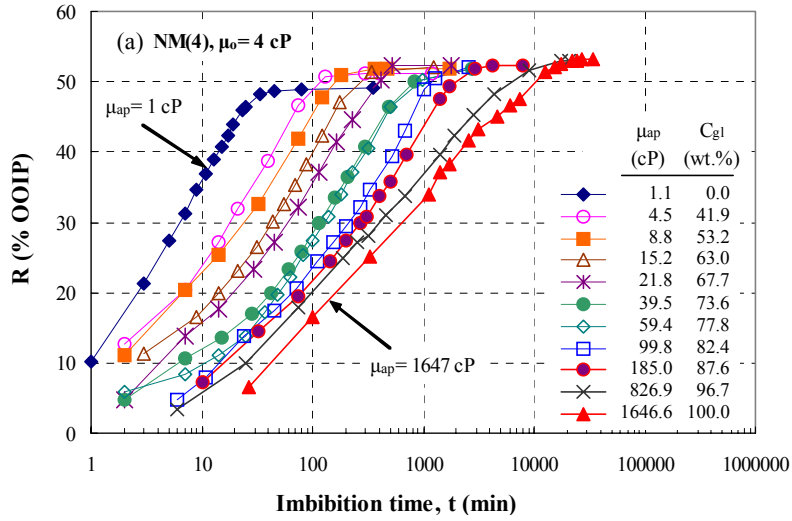


Fig. 4.1. Recovery of 4 cP oil by spontaneous imbibition for variation in aqueous phase viscosity versus (a) time and (b) dimensionless time; (c) final oil recovery,  $R_f$ , versus viscosity ratio.

Log-log plots of imbibition time versus viscosity ratio for specific normalized oil recoveries show close to parallel alignment (Fig. 4.2a). This kind of plot relates the time needed to recover a certain percentage of the total recoverable oil for a given viscosity ratio. Times for 100% (i.e. final) recovery are not identified because the recovery curves at late time are essentially asymptotic. The variation in  $t_D$  versus viscosity ratio, for different levels of recovery, illustrate the closeness to perfect scaling given by the geometric mean viscosity. (Fig. 4.2b). Overall there is a tendency for  $t_D$  to increase with viscosity ratio.

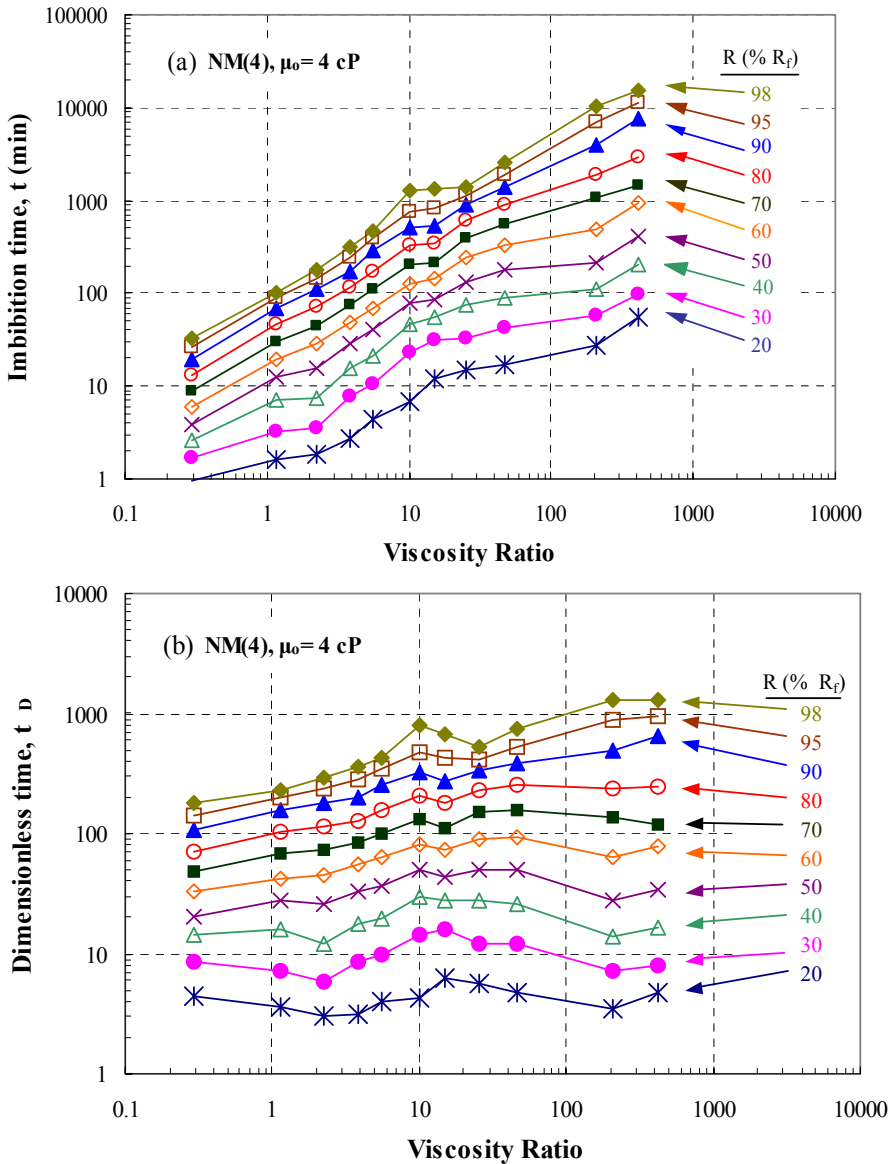


Fig. 4.2. Imbibition time (a) and dimensionless time (b) versus viscosity ratio ( $\mu_o = 4$  cP) for fractional recoveries,  $R$ , ranging from 20 % to 98 % (interpolated values for individual cores).

## Task 5. Comparison with similarity solutions.

### Introduction

The objective of Task 5 is to compare results given by simulation with special case analytic results given by similarity solutions for spontaneous imbibition for at least five distinct cases of rock and fluid properties.

### THEORY

The counter-current imbibition of a wetting phase against a non-wetting phase in a homogeneous porous medium is considered for the case in which the fluids are incompressible and immiscible. The motion is originated by preferential wettability and sustained by the capillary pressure gradient that results from the saturation gradient. Gravity effects are neglected. A mathematical model for this process is developed for the case of linear flow along the axis of a columnar sample of infinite length with the columnar surface sealed.

The Solution for the Saturation Profile

The basic equations governing counter-current imbibition flow are the generalized Darcy law

$$q_w = -\frac{Kk_{rw}A}{\mu_w} \frac{\partial P_w}{\partial x} \quad (5.1)$$

and

$$q_{nw} = -\frac{Kk_{rnw}A}{\mu_{nw}} \frac{\partial P_{nw}}{\partial x} \quad (5.2)$$

the capillary pressure definition

$$P_c = P_{nw} - P_w \quad (5.3)$$

the continuity of flow

$$q_w = -q_{nw} \quad (5.4)$$

and the conservation of mass equations

$$\phi A \frac{\partial S_w}{\partial t} + \frac{\partial q_w}{\partial x} = 0 \quad (5.5)$$

and

$$\phi A \frac{\partial S_{nw}}{\partial t} + \frac{\partial q_{nw}}{\partial x} = 0 \quad (5.6)$$

Combining equations 5.1 through 5.4 results in

$$q_w = \frac{K k_{rw} k_{rmw} A}{\mu_w k_{rmw} + \mu_{nw} k_{rw}} \frac{\partial Pc}{\partial x} \quad (5.7)$$

or in terms of saturation

$$q_w = \frac{K k_{rw} k_{rmw} A}{\mu_w k_{rmw} + \mu_{nw} k_{rw}} \frac{\partial Pc}{\partial S_w} \frac{\partial S_w}{\partial x} \quad (5.8)$$

Letting

$$M_w = \frac{K k_{rw} k_{rmw}}{\mu_w k_{rmw} + \mu_{nw} k_{rw}} \frac{\partial Pc}{\partial S_w} \quad (5.9)$$

then

$$q_w = M_w A \frac{\partial S_w}{\partial x} \quad (5.10)$$

Eq. (5.5) can be rewritten in terms of the classic “frontal advance theory.” At a fixed time, the derivative of the flow rate with position is given by

$$\left( \frac{\partial q_w}{\partial x} \right)_t = \left( \frac{\partial q_w}{\partial S_w} \right)_t \left( \frac{\partial S_w}{\partial x} \right)_t \quad (5.11)$$

$S_w$  is a function of both  $x$  and  $t$ . It follows that

$$dS_w = \left( \frac{\partial S_w}{\partial x} \right)_t dx + \left( \frac{\partial S_w}{\partial t} \right)_x dt \quad (5.12)$$

Consider the case where we wish to follow the movement of the location of a point with a given saturation. The locus of such a point is defined by setting the total differential of saturation equal to zero in Eq.5.11(5.12). After rearranging we obtain

$$\left( \frac{\partial S_w}{\partial t} \right)_x = - \left( \frac{\partial S_w}{\partial x} \right)_t \left( \frac{\partial x}{\partial t} \right)_{S_w} \quad (5.13)$$

Substituting Eqs. 5.11 and 5.13 into Eq. 5.5 and factoring out the common term

$$\left(\frac{\partial x}{\partial t}\right)_{S_w} = \frac{1}{\phi A} \left(\frac{\partial q_w}{\partial S_w}\right)_t \quad (5.14)$$

If the solution is self-similar, then the saturation profile must simply stretch along the  $x$ -direction with time. For such a stretching, the necessary condition is that

$$\left(\frac{\partial x}{\partial t}\right)_{S_w} = a(t) (S_{wo} - S_w) \quad (5.15)$$

where  $a(t)$  is a function of time and  $S_{wo}$  is the saturation at the open face. Combining Eqs. 5.14 and 5.15, and integrating

$$q_w = a(t) \phi A \left(S_{wo} - \frac{S_w}{2}\right) S_w + C \quad (5.16)$$

where  $C$  is a constant of integration.

Imbibition experiments can be run with an initial water saturation,  $S_{wi}$ , of almost any value. For example, initially the sample can be fully saturated with the non-wetting phase, or flooded to any saturation of non-wetting phase between the irreducible value and a value corresponding to the irreducible saturation of the wetting phase. Because flow is sustained by saturation gradients, the initial, constant saturation in the sample cannot result in any flow. It follows that the constant in Eq. 5.16 can be recovered by setting the flow rate at the initial saturation,  $S_{wi}$ , to zero. Therefore

$$C = -a(t) \phi A \left(S_{wo} - \frac{S_{wi}}{2}\right) S_{wi} \quad (5.17)$$

Combining Eqs. 5.10, 5.16 and 5.17

$$q_w = \frac{a(t) \phi A}{2} [(2S_{wo} - S_w) S_w - (2S_{wo} - S_{wi}) S_{wi}] \quad (5.18)$$

and

$$M_w \frac{\partial S_w}{\partial x} = \frac{a(t) \phi}{2} [(2S_{wo} - S_w) S_w - (2S_{wo} - S_{wi}) S_{wi}] \quad (5.19)$$

This location,  $x$ , for any value of saturation  $S_w$  at time  $t$ , can be found by integrating Eq. 5.19 to obtain

$$\int_{S_{wo}}^{S_w} \frac{2 M_w}{(2 S_{wo} - S_w) S_w - (2 S_{wo} - S_{wi}) S_{wi}} dS_w = a(t) \phi x \quad (5.20)$$

Eq. 5.20 does not have a general closed form solution due to the complexity of the  $M_s$  variable.

Because the profile is only stretched along the  $x$ -axis with time, the shape can be determined by making the  $x$ -variable arbitrary. That is, if the shape is all that is required, then  $a(t)\phi$  can be arbitrarily set to unity. The final results can then be scaled between 0 and  $x_f$ , the distance that the front has penetrated into the sample. This observation leads to the equation for the mean saturation. Selecting a time such that  $a(t)\phi = 1$ , Eq. 2.1-19 yields the relationship

$$dx^* = \frac{2 M_w}{[(2 S_{wo} - S_w) S_w - (2 S_{wo} - S_{wi}) S_{wi}]} dS_w \quad (5.21)$$

The average saturation is given by

$$\bar{S}_w = \frac{1}{x_f^*} \int_0^{x_f^*} S_w dx^* \quad (5.22)$$

where

$$x_f^* = \int_{S_{wo}}^{S_{wf}} \frac{2 M_w}{(2 S_{wo} - S_w) S_w - (2 S_{wo} - S_{wi}) S_{wi}} dS_w \quad (5.23)$$

Therefore

$$\bar{S}_w = \frac{\int_{S_{wo}}^{S_{wf}} \frac{2 M_w S_w}{(2 S_{wo} - S_w) S_w - (2 S_{wo} - S_{wi}) S_{wi}} dS_w}{\int_{S_{wo}}^{S_{wf}} \frac{2 M_w}{(2 S_{wo} - S_w) S_w - (2 S_{wo} - S_{wi}) S_{wi}} dS_w} \quad (5.24)$$

## CONCLUSIONS

1. Thin sections taken from different locations along a core after centrifuging gave saturations in the range of 58 to 76%.
2. Preliminary results on imbibition in pore models provided by consolidated beads showed unexpected variation in scaled imbibition rates.
3. Gas/oil and oil/brine imbibition data showed consistent features with respect to rate of frontal advance and dead end pressure behavior prior to when the front reaches the no-flow boundary
4. Correlated data for recovery of 4 cP oil showed a small but consistent increase in dimensionless time with increase in aqueous phase viscosity from 1 cP to 1650 cp. Residual saturations showed an overall decrease with increase in aqueous phase viscosity.
5. Imbibition saturation profile behavior can be described by an analytical solution.

## REFERENCES

- Bradford S., Leij F, “Estimating area for multi-fluid soil systems”, *Journal of Contaminant Hydrology*, 27 (1997) 83-105.
- Gladkikh M., Jain V., Bryant S., Sharma M.M., “Experimental and theoretical basis for a wettability-interfacial area-relative permeability relationship”, *SPE Annual Conference and Exhibition*, Denver, CO, USA, 5-8<sup>th</sup> October, 2003.
- Jain V., Bryant S., Sharma M.M., “Influence of wettability and saturation on liquid-liquid interfacial areas”, *Environ. Sci. Technol.* 2003, 37, 584-591.
- Kim H., Rao S.C., Annable M.D., “Determination of effective air-water interfacial area in partially saturated porous media using surfactant adsorption”, *Water Resources Research*, 33 , 2705-2711, Dec 1997.
- Ma, S., Zhang, X., Morrow, N.R., 1999. Influence of fluid viscosity on mass transfer between rock matrix and fractures. *Journal of Canadian Petroleum Technology*, v.38, no.7, pp.25-30.
- Ma, S., Morrow, N.R., Zhang, X., 1997. Generalized scaling of spontaneous imbibition data for strongly water-wet systems. *Journal of Petroleum Science and Engineering*, v.18, pp.165-178.
- Mattax, C.C., KYTE, J.R., 1962. Imbibition oil recovery from fractured, water-drive reservoir. *SPEJ*, June, pp.177-184.
- Morrow, N.R., “Physics and thermodynamics of capillary action in porous media”, *I&EC* 1970.

Scheafer C., DiCarlo D., Blunt M.J., “Determination of water –oil interfacial area during 3-phase gravity drainage in porous media”, *Journal of Colloid and Interface Science* 221, 308-312, 2000a.

Scheafer C., DiCarlo D., Blunt M.J., “Experimental measurement of air-water interfacial area during drainage and secondary imbibition in porous media” , *Water Resources Research*, 36 , 885-890, Apr 2000b.

Zhang, X., Morrow, N.R., MA, S., 1996. Experimental verification of a modified scaling group for spontaneous imbibition. *SPE Reservoir Engineering*, Nov., pp.280-285.